

## 가

1

. . . . . 2 . 2 . 3 . 4

: (acute renal failure; ARF)  
 (crescentic glomerulonephritis; CGN)  
 (acute tubular necrosis; ATN) 가 (MRI)  
 MRI ARF .  
 : 가 6 가 CGN 6  
 ATN 가 3  
 . CGN 1 , 4 , 7 , ATN  
 , 4 , 8 , 1 , 4 , 7 MRI MRI T1 T2  
 , MRI(dynamic MRI; DMRI)  
 . MRI  
 . MRI (sCr)  
 ,  
 : 가 T1, T2 -  
 DMRI . T1, T2  
 - ATN , CGN  
 sCr 가 , DMRI  
 : DMRI CGN ATN ARF 가  
 T1 T2 - ATN  
 CGN MRI ARF ATN CGN

가 (acute renal failure; ARF) 가 ATN RPGN  
 (acute tubular necrosis; ATN) 가 . CGN  
 (鎌狀) (crescentic glomerulonephritis; CGN) (chronic renal failure; CRF)  
 . CGN ATN 가 가  
 ARF ( 50-70% )  
 CGN (rapid progressive glomerulonephritis; RPGN) 가  
 가 가  
 가 ATN  
 . ATN 가

1  
2  
3  
4

1997

1999 1 6

1999 7 2

: 가

( )

가

가

가

CGN 가 6

가

가

가

(guinea pig) 100 µg

complete Freund's adjuvant (CFA)

(Sigma chemical Co., St. Louis, MO, U.S.A.)

가

. 2

incomplete Freund's adjuvant

(1, 2).

3-4

MRI

ga-

Ig G (guinea pig anti-rabbit GBM IgG) (University of Michigan Dr. Wiggins) . 100g

do- linium diethylene triamine pentaacetic acid( PA, Magnevist, Schering, Berlin Germany)

Gd-DT-

IgG (Sigma chemical Co., St. Louis, MO, U.S.A.)

MRI(dynamic MRI; DMRI)가

가

complete Freund's adjuvant (CFA)

(3-9)

. 5

가

RPGN

가

IgG 50mg

가

CGN

(10).

ATN

ATN 가 6

Ketamine hydrochloride (Ketalar,

MRI

, Seoul, Korea) 10-15mg/Kg Xylazine hydrochloride

(Rumpun,

, Seoul, Korea) 5 mg/Kg

(glycerol, Sig-ma, St. Louis, U.S.A.)

6.0mg/Kg

2.0-3.0 Kg

가 (New Zealand White rabbit)

(11).

2

3

3

가

7

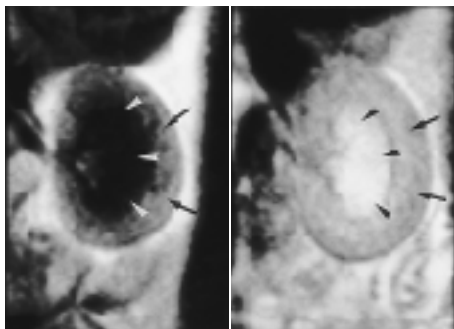
가

ARF 12

(ATN :6 , CGN :6 )

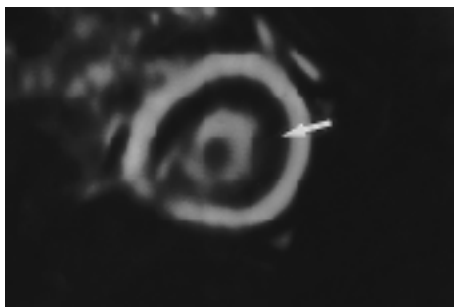
가 3

MRI 1.0T Magnetom Impact (Siemens, Erlan- gen, Germany) 가

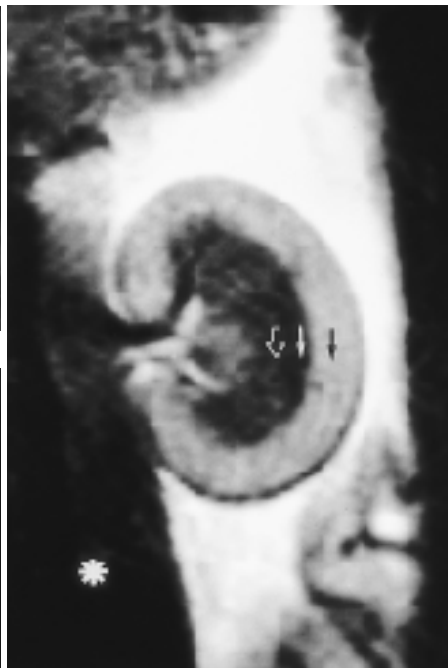


1A

1B



1C



2

Fig. 1. Normal renal MRI of the rabbit. T1-weighted (A) and T2-weighted (B) coronal image show normal cortex (arrows) and medulla (arrowheads). T1-weighted image show more distinct corticomedullary differentiation than that of the T2-weighted image. Gd-DT-PA enhanced renal dynamic MRI (C) shows intratubular passage of Gd-DT-PA as inwardly migrating dark band (arrow) pattern.

Fig. 2. Signal intensity were calculated from the circle of region of interest at three points-cortex (black arrow), outer (white arrow) and inner medulla (open arrow). Three times at nearest regions, and then relative signal intensity were calculated from signal intensity divided by signal intensity of adjacent back muscle (astract).

15 cm 20 cm  
MRI  
가  
T1  
400msec, 15msec, 200 × 256, 3  
4mm, 0.3mm, T2  
3000msec, 90msec, 200 × 256, 2  
4mm, 0.3mm  
(Fig. 1A, 1B).  
가  
Gd-DTPA 0.1mmol/Kg 가  
2-3 6ml  
FLASH(fast low angle shot sequence)  
T1 (fat suppression T1-weighted image:  
FST1WI) 36msec, 8msec, 50°  
128 × 256, 1, 0.5 cm 7  
40 ( : 4 40 )  
DMRI (Fig. 1C).  
MRI  
가  
(corticomedullary differentia-  
tion; CMD)  
DMRI  
MRI sCr  
CMD  
3 T1, T2  
(rela-

tive intensity) (Fig. 2), Terrier (12)  
(cortex to medulla contrast; CMC)  
(cortex to outer medulla contrast; COMC)  
(cortex to inner medulla contrast; CIMC)

Corticomedullary differentiation (CMD) :  
COMC and CIMC

COMC (%) (cortex to outer medulla contrast)

$$= \frac{I_c - I_{om}}{I_c + I_{om}} \times 100$$

I: relative intensity  
c: cortex  
om: outer medulla

CIMC (%) (cortex to inner medulla contrast)

$$= \frac{I_c - I_{im}}{I_c + I_{im}} \times 100$$

I: relative intensity  
c: cortex  
im: inner medulla

가 23 2ml  
sCr ATN  
(0), 4, 8, 1, 4, 7 sCr(mg/dl)  
CGN sCr  
가 4 8 (0)  
, 1, 4, 7 sCr 12  
Xylazine (5mg/Kg) Ketamin (10-15mg/Kg)  
20, 10cm

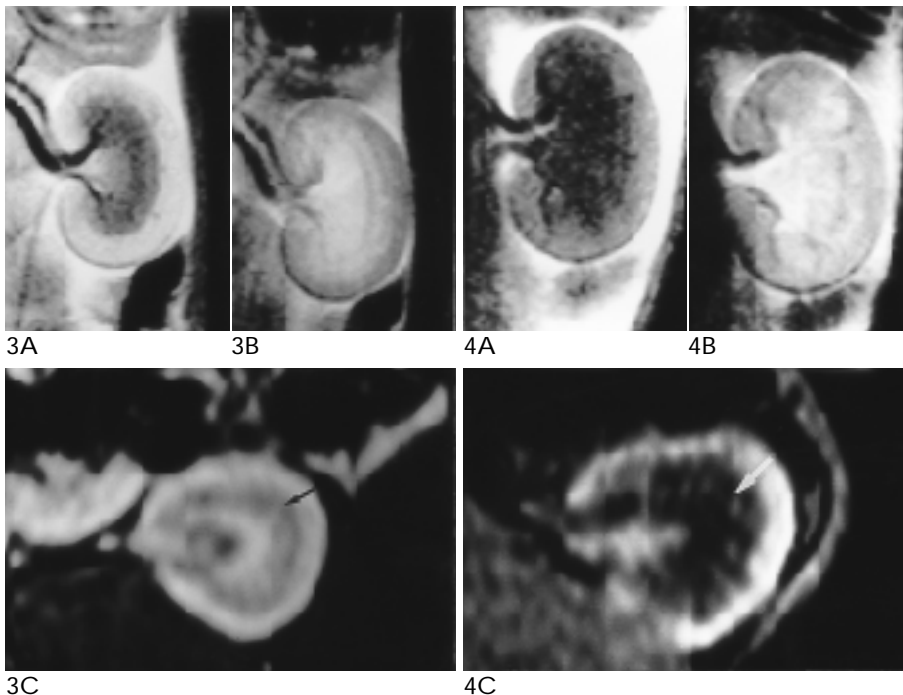


Fig. 3. Day one Acute Tubular Necrosis. Corticomedullary differentiation are well noted on T1-weighted (A) and T2-weighted (B) coronal image. Gd-DTPA enhanced renal dynamic MRI (C) well demonstrates a dark band (arrow) but weak signal intensity than normal.

Fig. 4. Day one Crescentic Glomerulonephritis. Corticomedullary differentiation are slightly obliterated on T1-weighted (A) and T2-weighted (B) coronal image.

Gd-DTPA enhanced renal dynamic MRI (C) shows poorly defined dark band (arrow) pattern.

: 가

(Angiomed, Karlsruhe, Germany)

가 (Table 1, 2).

7

MRI pentobarbital sodium (Entobar, , Seoul, Korea)

Hematoxylin & Eosin , ,

, sCr (mg/dl)

MRI COMC CIMC T1 T2

Non-parametric Friedman 95% (P<0.05) SPSS version 7.5

(Fig. 1A, B). ARF 가 , CGN ATN

24

(Fig. 3A, B) CMD가 T1 T2 , CGN(Fig. 4A, B) CMD T1, T2 ATN 4

CMD ATN(Fig. 5A, B) , CGN(Fig. 6A, B) , T2 7

ATN CGN MRI 4

(CMC); COMC CIMC

ARF가 ATN COMC

(P<0.001) T1 8.01 ± 9.90 , T2 -8.83 ± 7.24

(Table 1, 2). CGN COMC

T1 11.73 ± 8.45, T2 -7.88 ±

4.53 ATN COMC T1, T2

(P=0.051). CGN 가

(P<0.006). ATN CIMC

T1 19.57 ± 8.12, T2 -

8.18 ± 23.58 . CGN

CIMC T1 18.17 ± 8.80, T2

-11.83 ± 4.45 . ATN CIMC T1, T2

Creatinine (sCr)

가 sCr 1.2 ± 0.10mg/dl ARF

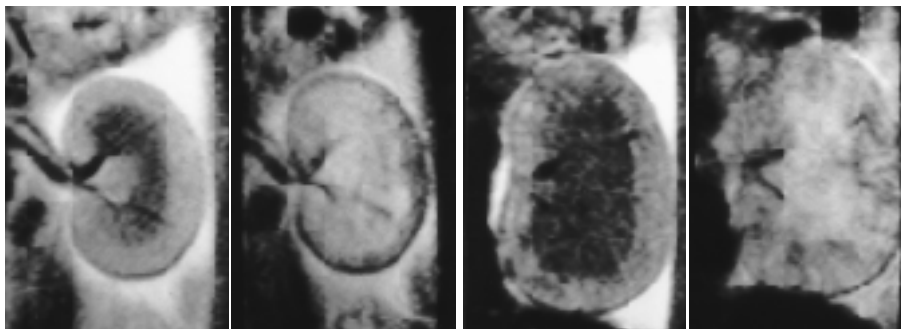
ATN CGN

가 . ATN

(P=0.57) CGN

(P<0.001). ATN 7

가 CGN

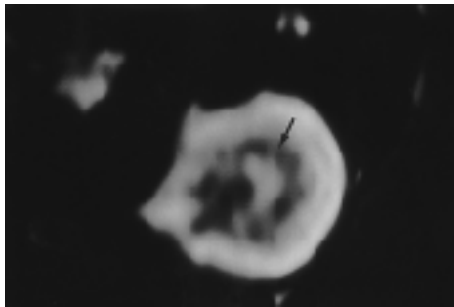


5A

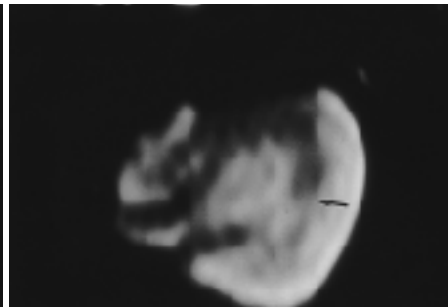
5B

6A

6B



5C



6C

Fig.5. Day four Acute Tubular Necrosis Corticomedullary differentiation and dark band (arrow) are relatively well defined in T1-weighted coronal image(A), T2-weighted coronal image(B), Gd-DTPA enhanced renal dynamic MRI(C).

Fig. 6. Day four Crescentic Glomerulonephritis.

Corticomedullary differentiation and dark band (arrow) are poorly defined, in T1-weighted coronal image(A), T2-weighted coronal image(B), Gd-DTPA enhanced renal dynamic MRI(C), especially in T2-weighted images.

Statistics	0 (n= 6)	4 hour (n= 6)	8 hour (n= 6)	24 hour (n= 6)	4 day (n= 6)	7 day (n= 6)	
Area(cm²)							
Coronal	6.5	6.8	6.9	7.4	7.7	7.9	*
Axial	3.5	3.7	3.8	3.9	3.95	4.5	*
sCr(mg/dl)	1.3	1.7	2.2	2	1.7	1.4	NS
COMC(%)							
T1	8.6	9.9	-1.2	6.8	6.5	5.1	NS
T2	-10.11	-11.14	-11.22	-10.37	-9.92	-7.9	NS, **
CIMC(%)							
T1	19.52	17.88	9.97	27.89	20.91	21.24	*
T2	-12.93	-19.04	-20.02	-19.19	-14.30	-9.43	NS, **

\* statistically significant, \*\*statistically significant in comparison with sCr

Statistics	0 (n= 6)	1 day (n= 6)	4 day (n= 6)	7 day (n= 6)	
Area(cm <sup>2</sup> )					
Coronal	7.2	7.7	8.8	9.3	*
Axial	4.3	4.3	4.9	5	*
sCr(mg/dl)	1.1	1.5	2.9	4.4	*
COMC(%)					
T1	11.87	13.09	8.62	-0.01	*, **
T2	-7.9	-6.25	-4.59	-2.89	*, **
CIMC(%)					
T1	18.31	23.75	20.42	12.16	*, **
T2	-11.86	-6.99	-9.69	-4.73	NS

\*\* statistically significant in comparison with sCr

DMRI  
가 DMRI Gd-DTPA

(Fig. 1C).

ARF

DMRI

ATN 4

DMRI

ATN (Fig. 3C) DMRI

24

CGN(Fig. 4C) DMRI

4

ATN (Fig. 6C).

5C), CGN

7 ATN CGN MRI 4

, sCr, CMD 가

ATN CGN

ATN

ARF 4

(Fig. 7),

1 ATN

가

4 ATN

7

. CGN 1

4 가

(Fig. 8) 7 가

(Bowman's space)

, 가

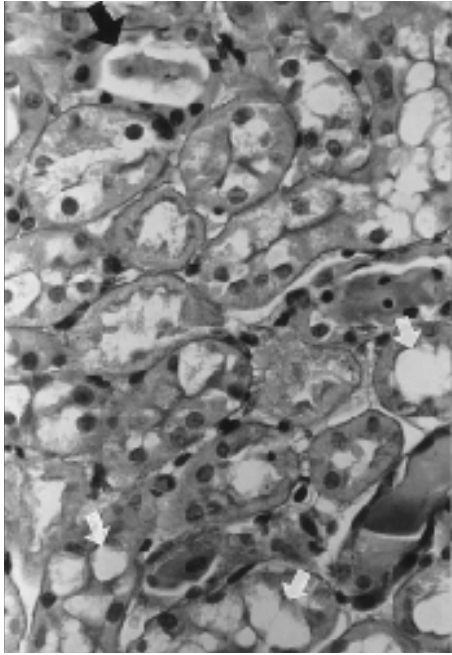
가

ARF

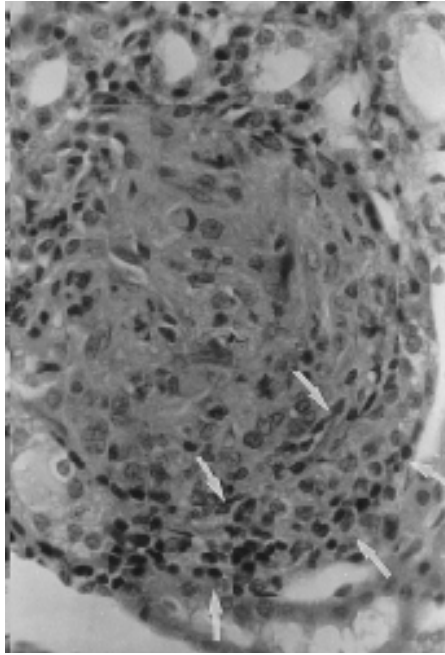
3

가 ARF

ARF



7



8

Fig. 7. Microphotography of Acute Tubular Necrosis at 4 hours.

Histologic findings shows tubule vacuolization (white arrows), sloughing and loss of nuclei of tubular cells and denuding portions of the tubular basement membrane (black arrow). Hematoxylin - Eosin stain, × 400

Fig. 8. Microphotography of Crescentic Glomerulonephritis at 4 days.

A glomerulus showing cellular crescent (white arrows) with markedly destroyed glomerular tuft and loss of Bowman's capsule. Bowman's space is obliterated by proliferated epithelial cells, spindle shaped cells and mononuclear cells. Hematoxylin - Eosin stain, × 100

가 6 ml/Kg

가 7 ATN 가

MRI (3, CGN Wiggins (10)

5, 13-15). DMRI 가가 MRI (9, 15-17). 가 DMRI Gd-DTPA가 ARF MRI 가 (28)

CMD (13, 18) 가 MRI

CMC가 가 CMC가 MRI (TR,TE),

T1 T2 (12). CMC (19). (20) CMC가 ,

가 (18, 20, 21). CMC가 CMC (12, 29-31)

ARF mercuric chloride ARF uranyl nitrate (21-24), (30) MRI 가 ARF

ARF (11, 25-27). ATN 10ml/Kg . ATN (16) 가 DMRI

가 , (17) ARF  
가 DMRI가 MRI (33) (30) 가  
가 , 가 CMC가 (26)  
DMRI - ARF (time-signal intensity curve) ATN  
(9) 가 CGN DMRI 2-24  
, sCr DMRI가 가 24  
CGN (34). (26) 가  
50% 70-80% ARF sCr 가  $3.0 \pm 0.5 \text{ mg/dl}$  ARF  
(2, 32). CGN 가 가  
CGN (9, ATN 가 DMRI  
14, 30). ARF MRI T2  
ATN MRI (20). ATN 4  
CGN ATN 가 가 (hemisiderin)  
가 가 ARF  
ATN ARF 가 CMC가 ,  
ATN ARF RPGN MRI 가 CGN  
CGN MRI 가 DMRI  
가 CMD 가  
CGN ARF ATN CGN  
가 ARF ATN , 가 MRI DMRI  
sCr 가 sCr가  
MRI ARF 가 가  
DMRI가 ARF 가 ATN ARF  
ATN 가 ARF CGN  
CGN ATN 가 ARF ATN CGN  
CRF 가 ARF  
가  
DMRI가  
ATN 가  
MRI T1 T2 가

1. Glassack RJ, Cohen AH, Adler SG. *Primary glomerular diseases*. In Brenner BM ed. *The kidney*. 5th ed. Philadelphia: Saunders 1995;1402-1411
2. Glassock RJ, Brenner BM. *The major glomeropathies*. In Isselbacher KJ, Braunwald E, Wilson JD, Martin JB, Fauci AS, Kasper DL, eds. *Harrison's principles of internal medicine*. 13th ed. St. Louis: McGraw-Hill, Inc. 1994;1303-1305
3. Carvlin MJ, Arger PH, Kundel HL, et al. Use of Gd-DTPA and fast gradient-echo and spin-echo MR imaging to demonstrate renal function in the rabbit. *Radiology* 1989;170:705-711

4. Kikinis R, von Schulthess GK, Jager P, et al. Normal and hydro-nephrotic kidney: evaluation of renal function with contrast-enhanced MR imaging. *Radiology* 1987;165:837-842
5. Semelka RC, Hricak H, Tomei E, et al. Obstructive nephropathy: evaluation with dynamic Gd-DTPA-enhanced MR imaging. *Radiology* 1990;175:797-803
6. Semelka RC, Corrigan K, Ascheer SM, et al. Renal cortico-medullary differentiation: observation in patient with differing serum creatinine levels. *Radiology* 1994;190:149-152
7. Haustein J, Niendorf HP, Krestin G, et al. Renal tolerance of gadolinium-DTPA/dimeglumine in patients with chronic renal failure. *Invest Radiol* 1992;27:153-156
8. Carvlin MJ, Arger PH, Dougherty L, et al. Dynamic renal MR imaging to investigate antglomerular basement membrane antibody-induced glomerulonephritis (abstr). *Radiology* 1987;165:85
9. . . 가  
Gd-DTPA .  
1998;38:319-327
10. Wiggins RC, Glatfelter A, Brukman J. Procoagulant activity in glomeruli and urine of rabbits with nephrotoxic nephritis. *Lab Invest* 1985;53:156-165
11. Oken DE, Arce ML, Wilson DR. Glycerol-induced hemoglobinuric acute renal failure in the rat. Micropuncture study of the development of oliguria. *J Clin Invest* 1966;45:724-735
12. Terrier F, Hricak H, Revel D, et al. Magnetic resonance imaging in the diagnosis of acute renal allograft rejection and its differentiation from acute tubular necrosis experimental study in the dog. *Invest Radiol* 1985;20:617-625
13. Hricak H, Crooks L, Sheldon F, Kaufman L. Nuclear magnetic resonance imaging of the kidney. *Radiology* 1983;146:425-432
14. Leung AW, Bydder GM, Steiner RE, et al. Magnetic resonance imaging of the kidneys. *AJR* 1984;143:1215-1227
15. Choyke PL, Frank JA, Gorton ME, et al. Dynamic Gd-DTPA-enhanced MR imaging of the kidney: experimental results. *Radiology* 1989;170:713-720
16. , , . 가  
Gd-DTPA 가 MRI .  
1994;30:893-900
17. , , : Gd-DTPA .  
1995;33:313-320
18. Choyke PL, Pollack HM. The role of MRI in disease of the kidney. *Radiol Clin North Am* 1988;26:617-631
19. Marotti M, Hricak H, Terrier F, McAninch JW, Thrurhoff JW. MR in renal disease: importance of cortical-medullary distinction. *Magn Reson Med* 1987;5:160-172
20. Kim SH, Kim S, Lee JS, et al. Hemorrhagic fever with renal syndrome: MR imaging of the kidney. *Radiology* 1990;175:823-825
21. Carvlin MJ, Arger PH, Kundel HL, et al. Acute tubular necrosis : use of Gadolinium-DTPA and fast MR imaging to evaluate renal function in the rabbit. *Radiology* 1989;170:705-711
22. Clark RL, Hillman BJ, Tracey P, Lee MS. Comparative microangiographic studies of glycerol- and mercuric chloride-induced acute renal failure in rats. *Invest Radiol* 1984;19:96-109
23. Munechika H, Sullivan DC, Hedlund LW, et al. Evaluation of acute renal failure with magnetic resonance imaging using gradient-echo and Gd-DTPA. *Invest Radiol* 1991;26:22-27
24. Yuasa Y, Kundel HL. Magnetic resonance imaging following unilateral occlusion of the renal circulation in the rabbits. *Radiology* 1985;154:151-156
25. de Miguel MH, Yeung HN, Goyal M, et al. Evaluation of quantitative magnetic resonance imaging as a noninvasive technique for measuring renal scarring in a rabbit model of antglomerular basement membrane disease. *J Am Soc Nephrol* 1994;4:1861-1868
26. . 가 Gd-DTPA  
MRI :  
1996
27. Carrol R, Kovacs K, Tapp E. The pathogenesis of glycerol-induced renal tubular necrosis. *J Path Bact* 1965;89:573-580
28. Kurtz TW, Maletz RM, Hsu CH. Renal cortical blood flow in glycerol-induced acute renal failure in the rat. *Circ Res.* 1975; 38:30-35
29. Rholl KS, Lee JKT, Ling D, et al. Acute renal rejection versus acute tubular necrosis in a canine model: MR evaluation. *Radiology* 1986;160:113-117
30. . 1993
31. Kundal HL, Schlakman B, Joseph PW, et al. Water content and N-MR relaxation time gradients in the rabbit kidney. *Invest Radiol* 1985; 21:12-17
32. Thomson MN, Holdsworth SR, Simpson IJ, Peters DK. Defibrination with ancrod in nephrotoxic nephritis in rabbits. *Kidney Int* 1976;10:343-347
33. Kim SH, Han MC, Kim S, Lee JS. Acute renal failure secondary to rhabdomyolysis: MR imaging of the kidney. *Acta Radiol* 1992; 33:1-4
34. Finckh ES. Experimental acute tubular necrosis following subcutaneous injection of glycerol. *J Pathol Bacteriol* 1957;73:69-85



## **A Comparative Study of MRI Findings of Experimentally Induced Rapid Progressive Glomerulonephritis (RPGN) and Acute Tubular Necrosis (ATN) in Rabbits<sup>1</sup>**

Ik Yang, M.D., Soo Young Chung, M.D., Kyung Won Lee, M.D., Yul Lee, M.D.,  
Eun Young Ko, M.D., Mi Sook Won, M. D., Jung Woo Noh, M.D.<sup>2</sup>,  
Roh Won Chun, M.D.<sup>2</sup>, Hyun Tae Kim, M.D.<sup>3</sup>, Moon Hyang Park, M.D.<sup>4</sup>

<sup>1</sup>Department of Radiology, Hallym University College of Medicine

<sup>2</sup>Department of Internal Medicine, Hallym University College of Medicine

<sup>3</sup>Department of Clinical Pathology, Hallym University College of Medicine

<sup>4</sup>Department of Pathology, Hanyang University College of Medicine

**Purpose :** To evaluate the usefulness of MR imaging in the differential diagnosis of the underlying causes of early-stage acute renal failure (ARF) by comparing the MRI findings of experimentally-induced crescentic glomerulonephritis (CGN) and acute tubular necrosis (ATN) in rabbits.

**Materials and Methods :** Experimental CGN was induced by injecting anti-glomerular basement membrane antibody into six rabbits, and ATN by injecting glycerol solution into six rabbits. A normal control group of three rabbits was also used. Renal MR imaging (T1- and T2-weighted coronal images and dynamic MRI : DMRI) was performed the day before, and one, four, and seven days after the induction of CGN; and immediately before, and four, and eight hours, and one, four, and seven days after the induction of ATN. Sequential renal gun-biopsies and blood sampling (serum creatinine, sCr) were performed. Renal area, corticomedullary differentiation (CMD), and the passage of Gd-DTPA (pattern of dark band), as seen on MRI, were analyzed and correlated with serial change of sCr.

**Results :** In normal kidneys, CMD was clearly apparent on both T1- and T2-weighted images. DMRI demonstrated a progressively inwardly migrating dark band in the kidneys. CMD was relatively clearly demonstrated in the ATN group but less clearly identified in the CGN group. Renal size (area) and sCr gradually increased in both the CGN and ATN groups, and dark bands were moderately to poorly defined in both.

**Conclusion :** We conclude that DMRI could be used to differentiate and evaluate disease processing and compromised renal function in cases of CGN and ATN. On T1- and T2-weighted images, CMD was relatively well preserved in the ATN group, but was less clear in the CGN group. These MRI findings may be helpful for differentiation of the underlying causes of early-stage ARF, particularly between CGN and ATN.

**Index words :** Animals

Kidney, inflammation

Kidney, MR

Address reprint requests to : Ik Yang, M.D., Department of Radiology, Kangnam Sacredheart Hospital, College of Medicine, Hallym University, #948-1, Daelim-1-dong, Youngdeungpo-ku, Seoul, 150-071, Korea.  
Tel. 82-2-829-5241, Fax. 82-2-832-1845